



Cite this: *New J. Chem.*, 2019, 43, 16123

Received 3rd August 2019,
Accepted 28th September 2019

DOI: 10.1039/c9nj04031e

rsc.li/njc

Facile synthesis of a 3D flower-like SiO₂-MOF architecture with copper oxide as a copper source for enantioselective capture†

Xinglin Li,^a Yu Gao,^a Cuijie Wang,^a Jiting Cui,^a Ajuan Yu^{ib}*^a and Shusheng Zhang^{ib}

A facile self-template synthetic approach for the facile synthesis of a 3D flower-like SiO₂-CuLBH architecture with copper oxide as a copper source has been demonstrated. The resulting composite as a sorbent showed a certain selective separation capability for phenyl methyl sulfoxide enantiomers (PMS) with an enantiomeric excess (ee) value of 31%.

Chirality is a unique property of chiral molecules, which plays an essential role in aspects of the medicine industry, food chemistry and drug manufacture.¹ Chiral compounds often exhibit different or opposite effects in terms of biological interaction, pharmacology and toxicity^{2,3} because of the difference in stereoscopic structure. Therefore, considering the importance and challenge of chiral separation, considerable chiral recognition materials and techniques have been developed.^{4–8} Solid phase extraction relying on chiral adsorbent materials has been proved to be the direct approach in obtaining optical isomers. Thus, it is crucial to develop novel chiral adsorbing materials for enantioselective adsorption.

In the last decade, metal-organic frameworks (MOFs) have emerged as promising materials by virtue of their structural diversity, well-defined open channels, molecular-sized cavities and so on. Apart from their potential applications in gas storage, catalysis, separation and sensing,^{9–11} MOFs are also ideally suited to serve as adsorbents and separators.¹² In particular, chiral MOF materials show great potential in asymmetric catalysts and enantioselective separations because of the chiral environment in the open channels of the framework.

Until now, composites have been proposed by combining MOF materials with other substrates, such as graphene oxide (GO),

Fe₃O₄, ZnO, precious metal nanoparticles, alumina and silica.^{13–18} MOF composites may have not only the outstanding performance of MOFs, but also the synergistic effects generated by two kinds of additives. Therefore, MOF composites are considered to be good adsorbents and separation materials for high-efficiency removal of targets. Silica materials tend to form functional composites¹⁹ mainly due to their high specific surface area, rich oxygen-containing groups and surface modifiable properties. Traditionally, the metal sources of MOFs are nitrate, acetate and other inorganic metallic salts, which will produce by-product anions such as Cl[−] and NO₃[−].^{20–22} They may constitute a safety hazard in industrial use and are also unfriendly to the environment. Therefore, an appealing alternative is to use metal oxides or metal hydroxide as metal sources for MOF building from safety and economic standpoints. Recently, metal oxides and hydroxides have been reported to act as sources of metal cations for MOF synthesis.^{23–27} However, to the best of our knowledge, there is no report using metal oxides and metal hydroxides as metal sources for the synthesis of chiral MOFs.

Herein, we adopt the strategy of a self-template synthetic approach for the facile synthesis of a 3D flower-like SiO₂-MOF ([Cu(*l*-mal)(bpy)]·H₂O) (SiO₂-CuLBH) architecture. First, silica spheres were prepared as a template to form a cupric oxide shell on their surface. Second, the cupric oxide shell served as the source of metal ions and was *in situ* converted to MOF, which made the composite present a structure similar to a “flower”. Then the enantioselective performance of the resulting composite SiO₂-CuLBH was evaluated by enantioselective adsorption of racemic phenyl methyl sulfoxide (PMS).

The morphology and structure of SiO₂-CuLBH was studied by scanning electron microscopy (SEM). As displayed in Fig. 1a, the prepared silica particles had a uniform size and good dispersion. The SEM image of SiO₂@CuO showed that the shells of the silica spheres became coarse due to the deposition of cupric oxide, although the distribution of copper oxide shell on the SiO₂ surface was not homogeneous (Fig. 2b). When *l*-(-)-malic acid and 4,4′-bipyridyl were added into the

^a College of Chemistry, Key Laboratory of Molecular Sensing and Harmful Substances Detection Technology, Zhengzhou University, Kexue Avenue 100, Zhengzhou, Henan 450001, P. R. China. E-mail: yuajuan@zzu.edu.cn

^b Center of Advanced Analysis and Computational Science, Key Laboratory of Molecular Sensing and Harmful Substances Detection Technology, Zhengzhou University, Kexue Avenue 100, Zhengzhou, Henan 450001, P. R. China

† Electronic supplementary information (ESI) available. See DOI: 10.1039/c9nj04031e

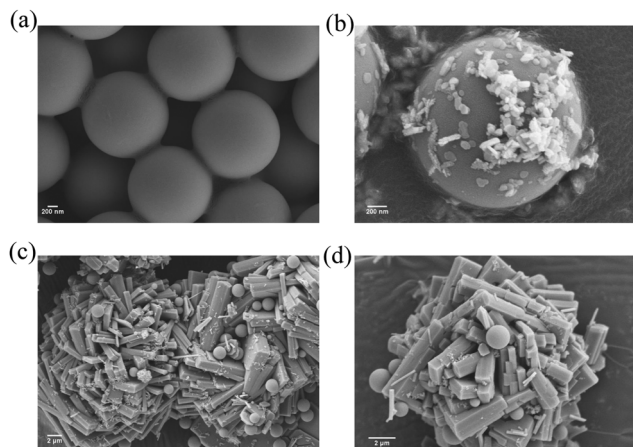


Fig. 1 SEM images of the as-prepared (a) 2.0 μm silica particles; (b) $\text{SiO}_2@\text{CuO}$; (c) and (d) $\text{SiO}_2\text{-CuLBH}$.

water/methanol solution of $\text{SiO}_2@\text{CuO}$, the color of the liquid changed from black to blue gradually, indicating the consumption of CuO and the formation of the CuLBH. The SEM of $\text{SiO}_2\text{-CuLBH}$ (Fig. 1c and d) indirectly exhibited this point. Compared with $\text{SiO}_2@\text{CuO}$, the consumption of CuO shell made the silica spheres smooth in $\text{SiO}_2\text{-CuLBH}$ and the composite presented a beautiful architecture similar to 3D “flowers”.

The reported CuLBH was synthesized in Teflon-lined steel bombs without physical stirring, but it's difficult to form homogeneous composites under these conditions. To address this problem, we modified the synthesis approach of CuLBH to use a round-bottomed flask in an oil bath with magnetic stirring. Powder X-ray diffraction (PXRD) (Fig. 2a) demonstrated that the skeleton structure of the MOF synthesized with the modified method was in agreement with the reported homochiral CuLBH synthesized in a Teflon-lined steel bomb. To demonstrate the successful synthesis of $\text{SiO}_2\text{-CuLBH}$, PXRD analysis was recorded. Fig. 2b presents the PXRD patterns of SiO_2 , $\text{SiO}_2@\text{CuO}$, CuLBH and $\text{SiO}_2\text{-CuLBH}$, respectively. The main diffraction peaks in the PXRD patterns with 2θ at 32.5° , 35.5° , 38.6° and 48.6° of CuO verified the existence of the CuO phase in the $\text{SiO}_2@\text{CuO}$. Furthermore, the diffraction intensity of specific peaks of CuO completely decreased and all of the pronounced diffraction peaks of CuLBH appeared in

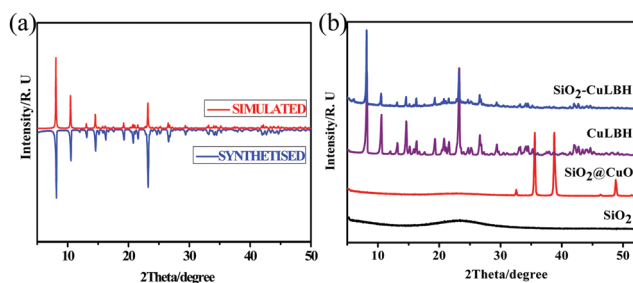


Fig. 2 (a) The experimental powder X-ray diffractogram of the as-synthesised CuLBH (inverted plot) and corresponding simulation result (normal plot); (b) PXRD patterns of SiO_2 , $\text{SiO}_2@\text{CuO}$, CuLBH and $\text{SiO}_2\text{-CuLBH}$.

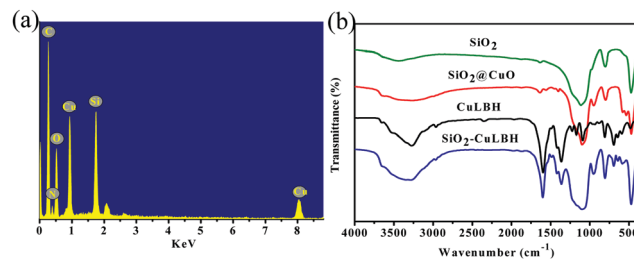


Fig. 3 (a) EDS result of $\text{SiO}_2\text{-CuLBH}$; (b) FT-IR spectra of SiO_2 , $\text{SiO}_2@\text{CuO}$, CuLBH and $\text{SiO}_2\text{-CuLBH}$.

$\text{SiO}_2\text{-CuLBH}$, which implied that the CuO shell was completely consumed and converted into CuLBH.

In addition, the energy dispersive X-ray (EDS) (Fig. 3a) of the composite also revealed the presence of Cu, Si, C, N, and O. The Fourier transform infrared (FT-IR) spectra are presented in Fig. 3b. In the FT-IR spectra of $\text{SiO}_2@\text{CuO}$, the signals of Si-O-Si at 1099 cm^{-1} , 947 cm^{-1} and the stretching vibration peaks of Cu-O at 587 cm^{-1} were observed, confirming that the CuO was coated onto the SiO_2 successfully. In the spectrum of CuLBH, the peaks at 3345 cm^{-1} , 2964 cm^{-1} and 1605 cm^{-1} corresponded to the O-H stretching vibration, C-H asymmetric stretching vibration and C=O asymmetric stretching vibration of L-malic acid, respectively. The peak at 808 cm^{-1} was the characteristic band of 4,4'-bipyridyl ligands. For $\text{SiO}_2\text{-CuLBH}$, it had both the characteristic absorption peak of SiO_2 and CuLBH. Besides, the absence of Cu-O characteristic absorption bands indicated the complete conversion of CuO into CuLBH *in situ*. Therefore, it could be suggested that the composite was successfully prepared. The thermogravimetric curves provide information concerning the thermal stability of the composite. As shown in Fig. S1 (ESI[†]), the weight loss of the $\text{SiO}_2\text{-CuLBH}$ composite occurred in the range from 100°C to 200°C , which was a result of the loss of the solvent molecule DMA. The decomposition of the organic ligand and the collapse of the structure occurred as the temperature increased up to 325°C , which showed that the material has good thermal stability.

Phenyl methyl sulfoxide (PMS) possesses two enantiomers of R-PMS and S-PMS, distributed in a racemic mixture. The enantioselective performance of $\text{SiO}_2\text{-CuLBH}$ was evaluated

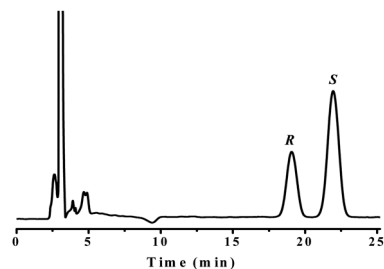


Fig. 4 The adsorption result for phenyl methyl sulfoxide (PMS). Conditions: Chiralpak IC column ($4.6 \times 250\text{ mm}$, $5\ \mu\text{m}$); mobile phase, hexane-isopropanol (80/20, v/v); flow rate, 0.6 mL min^{-1} ; detection wavelength, 254 nm ; column temperature, 25°C . The peaks that appeared before 10 minutes were the peaks of the extraction solvent (acetonitrile) and elution solvent (methanol).

by PMS and the enantiomeric composition of the separated enantiomer was analyzed by HPLC. As shown in Fig. 4, when acetonitrile and methanol were selected as the extraction solvent and elution solvent, an ee value of 31% was achieved for PMS. This result indicated that the stereo-selectivity of *S*-PMS was probably due to the most appropriate size and steric fit of SiO₂-CuLBH. To further demonstrate the superiority of the SiO₂-CuLBH composite for enantioselective capture of PMS, the selective adsorption ability of CuLBH which was synthesized in a Teflon-lined steel bomb, was also carried out under the same conditions for comparison. It is obvious that the ee value of 31% for PMS achieved by the prepared SiO₂-CuLBH showed a much higher response than CuLBH (with an ee value of 6%), which might be ascribed to the 3D flower-like architecture of SiO₂-CuLBH.

Conclusions

In summary, we have described a self-template synthetic approach for the facile preparation of a 3D flower-like SiO₂-CuLBH architecture, which served as a chiral adsorbent and was utilized for "enantioselective capture" of enantiomers. The results demonstrated that the prepared composite has a certain enantioselective capability for PMS, which was much more efficient than CuLBH conventionally synthesized in a Teflon-lined steel bomb. This research not only demonstrates the utilization of SiO₂-CuLBH for enantioselective capture of PMS racemate but also highlights the facile construction of a 3D flower-like chiral MOF architecture for enantioseparation.

Experimental

Preparation of [Cu(*L*-mal)(bpy)]·H₂O (CuLBH) crystals

[Cu(*L*-mal)(bpy)]·H₂O was synthesized according to methods from the literature.²⁸ Cu(OAc)₂·H₂O (0.090 g, 0.45 mmol), *L*-malic acid (0.123 g, 0.9 mmol) and 4,4'-bipyridyl (0.069 g, 0.45 mmol) were added into 9.0 mL of water/methanol mixture (1 : 1, v/v). The mixed solution was transferred to a 25 mL Teflon-lined stainless steel autoclave and heated at 100 °C for 24 h. The product was washed several times alternately with methanol and water, and dried in a vacuum oven to obtain [Cu(*L*-mal)(bpy)]·H₂O.

Preparation of SiO₂-CuLBH composite (Fig. S2, ESI[†])

SiO₂@CuO. 2.0 μm silica cores were prepared according to the literature.^{29,30} Briefly, 3.4 mL of TEOS, 3.3 mL of NH₃·H₂O, 9.9 mL of H₂O and 33.4 mL of ethanol were mixed under vigorous stirring. After 1 h, one-eighth of the sample was taken from the solution and employed as seeds for the subsequent growth of 1.2 μm SiO₂ spheres. In turn, one-fourth of the 1.2 μm SiO₂ sphere sample was removed and used as seeds for the growth of 2.0 μm SiO₂ spheres.

The SiO₂@CuO core-shell composite was prepared by the conventional coprecipitation method. 1.0 g of SiO₂ and 2.0 g of CuCl₂·2H₂O was added into 400 mL of ultrapure water and

ultrasonicated for 15 minutes, and then the pH was adjusted to 9.0–10.0 by 1.0 mol L⁻¹ of NaOH aqueous solution under vigorous stirring. The mixture was kept at 90 °C for 3 h. The product was washed sequentially with ultrapure water and ethanol, and dried in a vacuum oven overnight to obtain SiO₂@CuO.

SiO₂-CuLBH. 0.4 g SiO₂@CuO was added into 23 mL water/methanol (1 : 1, v/v) solution of *L*-(-)-malic acid (0.46 g, 3.5 mmol) and 4,4'-bipyridyl (0.27 g, 1.8 mmol). The mixture then was heated in an oil-bath at 110 °C for 24 h. The product was washed sequentially with ultrapure water and methanol, and dried in a vacuum oven overnight.

Chiral separation experiments

For extraction of PMS, racemic solution of PMS was added to 10 mL acetonitrile (final concentration 0.05 mg mL⁻¹), and then CuLBH (100 mg) or SiO₂-CuLBH (150 mg) was added. The mixture was stirred for 24 h to realize even dispersion, and then the mixture was centrifuged and the supernatants were removed. The collected composite-enantiomer complexes were mixed with 1 mL methanol and stirred for 12 h at room temperature in order to retrieve the absorbed enantiomers. Then the solution was collected *via* centrifugation and further filtrated through a 200 nm filter membrane. The resulting liquid was analyzed by HPLC with a Chiralpak IC column (4.6 × 150 mm, 5 μm), from which the enantiomeric excess (ee) value was obtained.

Conflicts of interest

There are no conflicts of interest to declare.

Acknowledgements

Financial support from the National Natural Science Foundation of China (21675144 and 21775140) is gratefully acknowledged.

Notes and references

- 1 Y. Liu, W. Xuan and Y. Cui, *Adv. Mater.*, 2010, **22**, 4112.
- 2 X. Kuang, Y. Ma, H. Su, J. Zhang, Y. B. Dong and B. Tang, *Anal. Chem.*, 2014, **86**, 1277.
- 3 X. Ma, W. R. Du, Y. Li, C. F. Hua, A. J. Yu, W. D. Zhao, S. S. Zhang and F. W. Xie, *J. Pharm. Biomed. Anal.*, 2019, **172**, 50.
- 4 B. Schuur, B. J. V. Verkuijl, A. J. Minnaard, J. G. de Vries, H. J. Heeres and B. L. Feringa, *Org. Biomol. Chem.*, 2011, **9**, 36.
- 5 W. J. Wang, X. L. Dong, J. P. Nan, W. Q. Jin, Z. Q. Hu, Y. F. Chen and J. W. Jiang, *Chem. Commun.*, 2012, **48**, 7022.
- 6 J. Y. Chan, H. C. Zhang, Y. Nolvachai, Y. X. Hu, H. J. Zhu, M. Forsyth, Q. F. Gu, D. E. Hoke, X. W. Zhang, P. J. Marriot and H. T. Wang, *Angew. Chem., Int. Ed.*, 2018, **57**, 17130.
- 7 M. Zhang, X. L. Chen, J. H. Zhang, J. Kong and L. M. Yuan, *Chirality*, 2016, **28**, 340.

- 8 D. D. Medina, J. Goldshtein, S. Margel and Y. Masta, *Adv. Funct. Mater.*, 2007, **17**, 944.
- 9 C. Y. Gao, H. R. Tian, J. Ai, L. J. Li, S. Dang, Y. Q. Lan and Z. M. Sun, *Chem. Commun.*, 2016, **52**, 11147.
- 10 C. Kutzscher, G. Nickerl, I. Senkovska, V. Bon and S. Kaskel, *Chem. Mater.*, 2016, **28**, 2573.
- 11 T. C. Wang, F. P. Doty, A. I. Benin, J. D. Sugar, W. L. York, E. W. Reinheimer, V. Stavila and M. D. Allendo, *Chem. Commun.*, 2019, **55**, 4647.
- 12 J. S. Zhao, H. W. Li, Y. Z. Han, R. Li, X. S. Ding, X. Feng and B. Wang, *J. Mater. Chem. A*, 2015, **3**, 12145.
- 13 Y. Gao, W. R. Du, A. J. Yu, X. L. Li, W. D. Zhao and S. S. Zhang, *Anal. Methods*, 2018, **10**, 5811.
- 14 X. Ma, X. H. Zhou, A. J. Yu, W. D. Zhao, W. F. Zhang, S. S. Zhang, L. L. Wei, D. J. Cook and A. Roy, *J. Chromatogr. A*, 2018, **1537**, 1.
- 15 F. Ke, L. G. Qiu, Y. P. Yuan, X. Jiang and J. F. Zhu, *J. Mater. Chem.*, 2012, **22**, 9497.
- 16 M. Jin, X. F. Qian, J. K. Gao, J. H. Chen, D. K. Hensley, H. C. Ho, R. J. Percoco, C. M. Ritzi and Y. F. Yue, *Inorg. Chem.*, 2019, **58**, 8332.
- 17 K. Huang, Z. Y. Dong, Q. Q. Li and W. Q. Jin, *Chem. Commun.*, 2013, **49**, 10326.
- 18 E. Zanchetta, L. Malfatti, R. Ricco, M. J. Styles, F. Lisi, C. J. Coghlan, C. J. Doonan, A. J. Hill, G. Brusatin and P. Falcaro, *Chem. Mater.*, 2015, **27**, 690.
- 19 S. Ehrling, C. Kutzscher, P. Freund, P. Müller, I. Senkovska and S. Kaskel, *Microporous Mesoporous Mater.*, 2018, **263**, 268.
- 20 J. Zhang, S. M. Chen, A. Zingiryan and X. H. Bu, *J. Am. Chem. Soc.*, 2008, **130**, 17246.
- 21 A. C. Kathalikkattil, P. S. Subramanian and E. Suresh, *Inorg. Chim. Acta*, 2011, **365**, 363.
- 22 J. Zhang, Y. G. Yao and X. H. Bu, *Chem. Mater.*, 2007, **19**, 5083.
- 23 J. B. Lin, R. B. Lin, X. N. Cheng, J. P. Zhang and X. M. Chen, *Chem. Commun.*, 2011, **47**, 9185.
- 24 G. Majano and J. P. Ramírez, *Adv. Mater.*, 2013, **25**, 1052.
- 25 Y. G. Liu, S. H. Li, X. F. Zhang, H. O. Liu, J. S. Qiu, Y. S. Li and K. L. Yeung, *Chem. Commun.*, 2014, **48**, 77.
- 26 Y. F. Yue, Z. A. Qiao, X. F. Li, A. J. Binder, E. Formo, Z. W. Pan, C. C. Tian, Z. H. Bi and S. Dai, *Cryst. Growth Des.*, 2013, **13**, 1002.
- 27 J. J. Zhao, W. T. Nunn, P. C. Lemaire, Y. L. Lin, M. D. Dickey, C. J. Oldham, H. J. Walls, G. W. Peterson, M. D. Losego and G. N. Parsons, *J. Am. Chem. Soc.*, 2015, **137**, 13756.
- 28 M. S. Zavakhina, D. G. Samsonenko, A. V. Virovets and D. N. Dybtsev, *J. Solid State Chem.*, 2014, **210**, 125.
- 29 J. O. Omamoghosa, J. P. Hanrahan, J. Tobin and J. D. Glennon, *J. Chromatogr. A*, 2011, **1218**, 1942.
- 30 Q. S. Qu, Y. Min, L. H. Zhang, Q. Xu and Y. D. Yin, *Anal. Chem.*, 2015, **87**, 9631.